Julius-Maximilians-UNIVERSITÄT WÜRZBURG

NLO EW corrections to polarised $W^+ W^-$ production and decay at the LHC

Christoph Haitz
in collaboration with Ansgar Denner and Giovanni Pelliccioli

Institut für Theoretische Physik 2
Julius-Maximilians-Universität Würzburg

29.02.2024

based on arXiv:2311.16031 (accepted by Physics Letters B)

Motivation

- Polarised processes allow for deep insights into spontaneous symmetry breaking
- Polarised cross-sections are very sensitive to beyond-Standard Model effects
- Polarisation is well suited for tests of the Standard Model

Existing work on polarised W^+W^- production

- Theoretical studies of polarised W^+W^- production in the double-pole approximation
  - NLO QCD, Denner and Pellicciioli 2020, arXiv:2006.14867 [1]
  - NNLO QCD Poncelet and Popescu 2021, arXiv:2102.13583 [2]
  - NLO QCD + parton showers Pelliccioli and Zanderighi 2023, arXiv:2311.05220 [3]
  - So far no calculation of the NLO EW corrections
- So far no experimental polarisation studies of W^+W^- production exist
  - Most difficult di-boson production process to observe (2 final state neutrinos)
  - Feasible with the data from the LHC run-3 and LHC HL-run

Definition of cross-sections with polarised intermediate vector-bosons

- The double-pole approximation is used to define polarised cross-sections
  - Non resonant contributions are removed
  - Polarisation is defined at the amplitude level
  - Polarised amplitude is used to calculate polarised cross-sections

Setup

$$p\,p \to W^+(\to e^+\,\nu_e)\,W^-(\to \mu^-\overline{\nu}_\mu) + X$$

- Calculate NLO EW corrections, Denner et al. 2023, arXiv:2311.16031 [4]
- The W bosons decay into different flavour leptons
- Polarisation is defined in the center-of-mass frame of the two bosons
- Assume perfect bottom-jet veto

- Analog calculation of the NLO EW and QCD corrections. Dao and Le 2023, arXiv:2311.17027 [5]

Phase-space cuts

- Charged leptons are dressed with the anti-k_T algorithm ($R = 0.1$)

Single lepton cuts	min p_{T,l_1}	25 GeV
	min p_{T,l_2}	20 GeV
	max $\lvert\eta_{e^+}\rvert$	2.5
	max $\lvert\eta_{\mu^-}\rvert$	2.4
charged lepton pair cuts	min $p_{T,e^+\mu^-}$	30 GeV
	min $M_{e^+\mu^-}$	20 GeV
Missing momentum cut	min $p_{T,mis}$	20 GeV

Integrated results

state	σ_{LO} [fb]	$\sigma_{\mathrm{NLO\,EW}}$ [fb]	δ_{EW}[%]	f_{NLO}[%]	σ_{LO} [fb]	$\sigma_{\mathrm{NLO\,EW}}$ [fb]	δ_{EW}[%]	f_{NLO}[%]
	$b\bar{b}$ excluded				$b\bar{b}$ included			
full	254.79(2)	249.88(9)	−1.93	103.5	259.02(2)	253.95(9)	−1.96	103.4
unp.	245.79(2)	241.48(2)	−1.75	100	249.97(2)	245.49(2)	−1.79	100.0
LL	18.752(2)	18.510(2)	−1.30	7.7	21.007(2)	20.663(2)	−1.64	8.4
LT	32.084(3)	32.043(3)	−0.13	13.3	33.190(3)	33.115(3)	−0.23	13.5
TL	33.244(5)	33.155(5)	−0.27	13.7	34.352(5)	34.230(5)	−0.35	13.9
TT	182.17(2)	177.83(2)	−2.38	73.6	182.56(2)	178.21(3)	−2.38	72.6
int.	−20.46(3)	−20.1(1)	−1.96	−8.3	−21.14(5)	−20.6(2)	−2.45	−8.4

(...) Monte-Carlo uncertainty

Integrated results

state	σ_{LO} [fb]	$\sigma_{NLO\,EW}$ [fb]	δ_{EW}[%]	f_{NLO}[%]	σ_{LO} [fb]	$\sigma_{NLO\,EW}$ [fb]	δ_{EW}[%]	f_{NLO}[%]
	$b\bar{b}$ excluded				$b\bar{b}$ included			
full	254.79(2)	249.88(9)	−1.93	103.5	259.02(2)	253.95(9)	−1.96	103.4
unp.	245.79(2)	241.48(2)	−1.75	100	249.97(2)	245.49(2)	−1.79	100.0
LL	18.752(2)	18.510(2)	−1.30	7.7	21.007(2)	20.663(2)	−1.64	8.4
LT	32.084(3)	32.043(3)	−0.13	13.3	33.190(3)	33.115(3)	−0.23	13.5
TL	33.244(5)	33.155(5)	−0.27	13.7	34.352(5)	34.230(5)	−0.35	13.9
TT	182.17(2)	177.83(2)	−2.38	73.6	182.56(2)	178.21(3)	−2.38	72.6
int.	−20.46(3)	−20.1(1)	−1.96	−8.3	−21.14(5)	−20.6(2)	−2.45	−8.4

- Difference between full off-shell calculation and the double-pole approximated calculation is $\approx 3.5\%$ (expected Γ_W/M_W)

Integrated results

state	σ_{LO} [fb]	$\sigma_{NLO\,EW}$ [fb]	$\delta_{EW}[\%]$	$f_{NLO}[\%]$	σ_{LO} [fb]	$\sigma_{NLO\,EW}$ [fb]	$\delta_{EW}[\%]$	$f_{NLO}[\%]$
	$b\bar{b}$ excluded				$b\bar{b}$ included			
full	254.79(2)	249.88(9)	−1.93	103.5	259.02(2)	253.95(9)	−1.96	103.4
unp.	245.79(2)	241.48(2)	−1.75	100	249.97(2)	245.49(2)	−1.79	100.0
LL	18.752(2)	18.510(2)	−1.30	7.7	21.007(2)	20.663(2)	−1.64	8.4
LT	32.084(3)	32.043(3)	−0.13	13.3	33.190(3)	33.115(3)	−0.23	13.5
TL	33.244(5)	33.155(5)	−0.27	13.7	34.352(5)	34.230(5)	−0.35	13.9
TT	182.17(2)	177.83(2)	−2.38	73.6	182.56(2)	178.21(3)	−2.38	72.6
int.	−20.46(3)	−20.1(1)	−1.96	−8.3	−21.14(5)	−20.6(2)	−2.45	−8.4

- Including bottom antibottom induced processes enhances the production of longitudinally polarised W bosons
- Diagrams with t channel top quarks
- Top quark predominantly couples to longitudinally polarised W bosons

Angular separation positron and muon $\cos(\Delta\vartheta_{e^+\mu^-}) = \frac{\vec{p}_{e^+}\vec{p}_{\mu^-}}{|\vec{p}_{e^+}||\vec{p}_{\mu^-}|}$

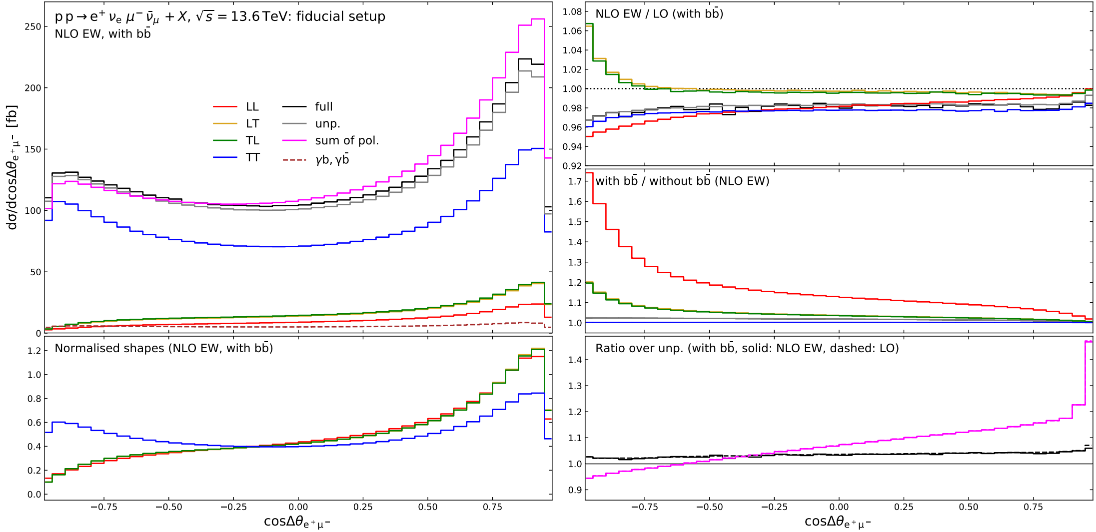

Angular separation positron and muon $\cos(\Delta\vartheta_{e^+\mu^-}) = \frac{\vec{p}_{e^+}\vec{p}_{\mu^-}}{|\vec{p}_{e^+}||\vec{p}_{\mu^-}|}$

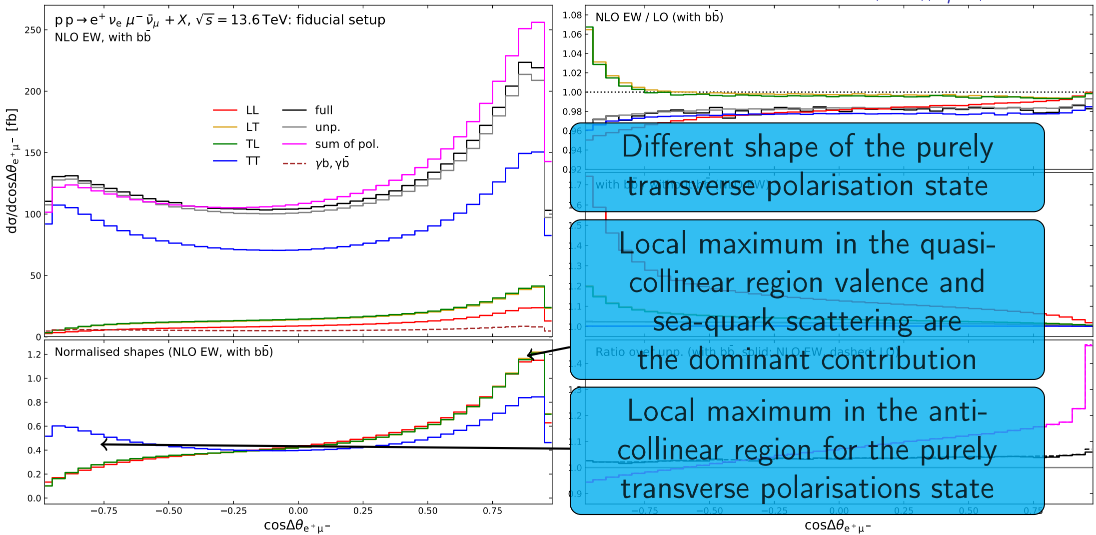

Different shape of the purely transverse polarisation state

Local maximum in the quasi-collinear region valence and sea-quark scattering are the dominant contribution

Local maximum in the anti-collinear region for the purely transverse polarisations state

Summary

- Calculated the polarised cross-sections for W^+W^- production at NLO EW
  - Used the double-pole approximation to define polarised W^+W^- production
  - Used methods are essential to the calculation of the NLO EW corrections to the decay of other charged resonances
    - Polarisation studies of vector-boson scattering processes
- Unobservable neutrinos in the final state make the distinction of the polarisation states more difficult
  - Less suitable observables compared to ZZ production

Bibliography I

- A. Denner and G. Pelliccioli, *Polarized electroweak bosons in W^+W^- production at the LHC including NLO QCD effects*, *JHEP* **09** (2020) 164, [arXiv:2006.14867].
- R. Poncelet and A. Popescu, *NNLO QCD study of polarised W^+W^- production at the LHC*, *JHEP* **07** (2021) 023, [arXiv:2102.13583].
- G. Pelliccioli and G. Zanderighi, *Polarised-boson pairs at the LHC with NLOPS accuracy*, arXiv:2311.05220.
- A. Denner, C. Haitz, and G. Pelliccioli, *NLO EW corrections to polarised W^+W^- production and decay at the LHC*, arXiv:2311.16031.
- T. N. Dao and D. N. Le, *NLO electroweak corrections to doubly-polarized W^+W^- production at the LHC*, arXiv:2311.17027.

Backup Slides

Definition of cross-sections with polarised intermediate vector-bosons

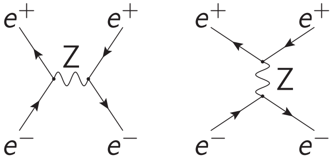

- Diagrams with and without the wanted (s-channel) resonance contribute to a given process
- Remove non-resonant diagrams in a gauge-independent way
  - This can be achieved by using a pole approximation
    - ⋆ Set resonant particles on-shell $\{p_i\} \Rightarrow \{\tilde{p}_i\}$
    - ⋆ Conserve some off-shell effects by using the off-shell denominators of the propagators and applying the phase-space cuts to the off-shell momenta

$$M\left(\{\tilde{p}\}, p_{res}^2\right) = M_{\mu,\text{production}}\left(\{\tilde{p}\}\right)\frac{N^{\mu\nu}\left(\{\tilde{p}\}\right)}{p_{res}^2 - m^2 + im\Gamma}M_{\nu,\text{decay}}\left(\{\tilde{p}\}\right)$$

Definition of cross-sections with polarised intermediate vector-bosons

- Numerator of the resonant propagator contains a sum over all polarisation states

$$\sum_{\text{polarisations}} \epsilon^{*}_{\mu}\epsilon_{\nu} = -g_{\mu\nu} \quad \text{(Feynman-´t Hooft gauge)}$$

$$M\left(\{\tilde{p}\}, p^2_{res}\right) = \sum_{\lambda} M_{\mu,\text{production}}\left(\{\tilde{p}\}\right) \frac{\epsilon^{\mu *}_{\lambda}\left(\{\tilde{p}\}\right)\epsilon^{\nu}_{\lambda}\left(\{\tilde{p}\}\right)}{p^2_{res} - m^2 + im\Gamma} M_{\nu,\text{decay}}\left(\{\tilde{p}\}\right)$$

$$M\left(\{\tilde{p}\}, p^2_{res}\right) = \sum_{\lambda} M_{\lambda}\left(\{\tilde{p}\}, p^2_{res}\right)$$

Definition of cross-sections with polarised intermediate vector-bosons

- Take the square of the matrix element to calculate the cross-section

$$\underbrace{\left|M\left(\{\tilde{p}\}, p_{res}^2\right)\right|^2}_{\text{unpolarised}} = \sum_{\lambda} \underbrace{\left|M_\lambda\left(\{\tilde{p}\}, p_{res}^2\right)\right|^2}_{\text{polarisation } \lambda} + \underbrace{\sum_{\lambda \neq \lambda'} M_\lambda^*\left(\{\tilde{p}\}, p_{res}^2\right) M_{\lambda'}\left(\{\tilde{p}\}, p_{res}^2\right)}_{\text{interferences}}$$

NLO EW corrections with charged resonances

- Diagrams with real radiation from the resonant propagators contribute
- To preserve gauge invariance the decay width of the resonant particle is set to zero everywhere but in the resonant propagators
- This results in additional divergences not present in the full off-shell calculation
  - Divergence is split between the production and decay part
  - Additional local counterterms (massive dipoles) are needed to cancel the infrared divergences

Partial fraction decomposition

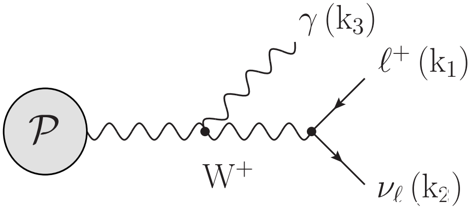

$$\mathcal{A}_{\text{prop}} = \mathcal{N}_{\text{prop}}(k_1, k_2, k_3)\,\frac{1}{s_{123} - M_W^2 + iM_W\Gamma_W} \cdot \frac{1}{s_{12} - M_W^2 + iM_W\Gamma_W}$$
$$= -\frac{\mathcal{N}_{\text{prop}}(k_1, k_2, k_3)}{s_{13} + s_{23}}\left(\frac{1}{s_{123} - M_W^2 + iM_W\Gamma_W} - \frac{1}{s_{12} - M_W^2 + iM_W\Gamma_W}\right)$$

- Use a partial fraction decomposition to split the divergence between the process where the photon is emitted from the production and from the decay amplitude

Partial fraction decomposition

- Project s_{12} on-shell $\rightarrow$ divergence is only in the production amplitude

$$\tilde{\mathcal{A}}^{(2)}_{\mathrm{prop}} = \frac{1}{s_{12} - M_\mathrm{W}^2 + iM_\mathrm{W}\Gamma_\mathrm{W}} \left[\frac{\mathcal{N}_{\mathrm{prop}}(\tilde{k}_1^{(12)}, \tilde{k}_2^{(12)}, \tilde{k}_3^{(12)})}{\tilde{s}_{13}^{(12)} + \tilde{s}_{23}^{(12)}} \right]$$

- Project s_{123} on-shell $\rightarrow$ divergence is only in the decay amplitude

$$\tilde{\mathcal{A}}^{(3)}_{\mathrm{prop}} = \frac{1}{s_{123} - M_\mathrm{W}^2 + iM_\mathrm{W}\Gamma_\mathrm{W}} \left[- \frac{\mathcal{N}_{\mathrm{prop}}(\tilde{k}_1^{(123)}, \tilde{k}_2^{(123)}, \tilde{k}_3^{(123)})}{\tilde{s}_{13}^{(123)} + \tilde{s}_{23}^{(123)}} \right]$$

- Massive particle counterterms can be used to cancel the divergences in the production and decay amplitude

Integrated results

state	σ_{LO} [fb]	$\sigma_{NLO\,EW}$ [fb]	δ_{EW}[%]	f_{NLO}[%]	σ_{LO} [fb]	$\sigma_{NLO\,EW}$ [fb]	δ_{EW}[%]	f_{NLO}[%]
	$b\bar{b}$, γb, $\gamma\bar{b}$ excluded				$b\bar{b}$ included, γb, $\gamma\bar{b}$ excluded			
full	254.79(2)	249.88(9)	−1.93	103.5	259.02(2)	253.95(9)	−1.96	103.4
unp.	245.79(2)	241.48(2)	−1.75	100	249.97(2)	245.49(2)	−1.79	100.0
LL	18.752(2)	18.510(2)	−1.30	7.7	21.007(2)	20.663(2)	−1.64	8.4
LT	32.084(3)	32.043(3)	−0.13	13.3	33.190(3)	33.115(3)	−0.23	13.5
TL	33.244(5)	33.155(5)	−0.27	13.7	34.352(5)	34.230(5)	−0.35	13.9
TT	182.17(2)	177.83(2)	−2.38	73.6	182.56(2)	178.21(3)	−2.38	72.6
int.	−20.46(3)	−20.1(1)	−1.96	−8.3	−21.14(5)	−20.6(2)	−2.45	−8.4
	$b\bar{b}$, γb, $\gamma\bar{b}$ included							
full	259.02(2)	265.59(9)	+2.54	-				

(...) Monte-Carlo uncertainty

Integrated results

state	σ_{LO} [fb]	$\sigma_{\mathrm{NLO\,EW}}$ [fb]	$\delta_{\mathrm{EW}}[\%]$	$f_{\mathrm{NLO}}[\%]$	σ_{LO} [fb]	$\sigma_{\mathrm{NLO\,EW}}$ [fb]	$\delta_{\mathrm{EW}}[\%]$	$f_{\mathrm{NLO}}[\%]$
	$\mathrm{b\bar{b}}$, $\gamma\mathrm{b}$, $\gamma\mathrm{\bar{b}}$ excluded				$\mathrm{b\bar{b}}$ included, $\gamma\mathrm{b}$, $\gamma\mathrm{\bar{b}}$ excluded			
full	254.79(2)	249.88(9)	-1.93	103.5	259.02(2)	253.95(9)	-1.96	103.4
unp.	245.79(2)	241.48(2)	-1.75	100	249.97(2)	245.49(2)	-1.79	100.0
LL	18.752(2)	18.510(2)	-1.30	7.7	21.007(2)	20.663(2)	-1.64	8.4
LT	32.084(3)	32.043(3)	-0.13	13.3	33.190(3)	33.115(3)	-0.23	13.5
TL	33.244(5)	33.155(5)	-0.27	13.7	34.352(5)	34.230(5)	-0.35	13.9
TT	182.17(2)	177.83(2)	-2.38	73.6	182.56(2)	178.21(3)	-2.38	72.6
int.	$-20.46(3)$	$-20.1(1)$	-1.96	-8.3	$-21.14(5)$	$-20.6(2)$	-2.45	-8.4
	$\mathrm{b\bar{b}}$, $\gamma\mathrm{b}$, $\gamma\mathrm{\bar{b}}$ included							
full	259.02(2)	265.59(9)	$+2.54$	-				

- Difference between full off-shell calculation and the double-pole approximated calculation is $\approx 3.5\%$ (expected Γ_W/M_W)

Integrated results

state	σ_{LO} [fb]	$\sigma_{NLO\,EW}$ [fb]	δ_{EW}[%]	f_{NLO}[%]	σ_{LO} [fb]	$\sigma_{NLO\,EW}$ [fb]	δ_{EW}[%]	f_{NLO}[%]
	$b\bar{b}$, γb, $\gamma\bar{b}$ excluded				$b\bar{b}$ included, γb, $\gamma\bar{b}$ excluded			
full	254.79(2)	249.88(9)	−1.93	103.5	259.02(2)	253.95(9)	−1.96	103.4
unp.	245.79(2)	241.48(2)	−1.75	100	249.97(2)	245.49(2)	−1.79	100.0
LL	18.752(2)	18.510(2)	−1.30	7.7	21.007(2)	20.663(2)	−1.64	8.4
LT	32.084(3)	32.043(3)	−0.13	13.3	33.190(3)	33.115(3)	−0.23	13.5
TL	33.244(5)	33.155(5)	−0.27	13.7	34.352(5)	34.230(5)	−0.35	13.9
TT	182.17(2)	177.83(2)	−2.38	73.6	182.56(2)	178.21(3)	−2.38	72.6
int.	−20.46(3)	−20.1(1)	−1.96	−8.3	−21.14(5)	−20.6(2)	−2.45	−8.4
	$b\bar{b}$, γb, $\gamma\bar{b}$ included							
full	259.02(2)	265.59(9)	+2.54	-				

- Including the photon bottom/antibottom induced processes adds a background from top W production
- This background would have to be subtracted with a fit in a polarisation analysis

Integrated results

state	σ_{LO} [fb]	$\sigma_{\mathrm{NLO\,EW}}$ [fb]	δ_{EW}[%]	f_{NLO}[%]	σ_{LO} [fb]	$\sigma_{\mathrm{NLO\,EW}}$ [fb]	δ_{EW}[%]	f_{NLO}[%]
	$\mathrm{b\bar{b}}$, γb, $\gamma\bar{\mathrm{b}}$ excluded				$\mathrm{b\bar{b}}$ included, γb, $\gamma\bar{\mathrm{b}}$ excluded			
full	254.79(2)	249.88(9)	-1.93	103.5	259.02(2)	253.95(9)	-1.96	103.4
unp.	245.79(2)	241.48(2)	-1.75	100	249.97(2)	245.49(2)	-1.79	100.0
LL	18.752(2)	18.510(2)	-1.30	7.7	21.007(2)	20.663(2)	-1.64	8.4
LT	32.084(3)	32.043(3)	-0.13	13.3	33.190(3)	33.115(3)	-0.23	13.5
TL	33.244(5)	33.155(5)	-0.27	13.7	34.352(5)	34.230(5)	-0.35	13.9
TT	182.17(2)	177.83(2)	-2.38	73.6	182.56(2)	178.21(3)	-2.38	72.6
int.	$-20.46(3)$	$-20.1(1)$	-1.96	-8.3	$-21.14(5)$	$-20.6(2)$	-2.45	-8.4
	$\mathrm{b\bar{b}}$, γb, $\gamma\bar{\mathrm{b}}$ included							
full	259.02(2)	265.59(9)	$+2.54$	-				

- NLO EW corrections are negative
- Corrections are smaller for the mixed polarisation states

Integrated results

state	σ_{LO} [fb]	$\sigma_{\mathrm{NLO\,EW}}$ [fb]	δ_{EW}[%]	f_{NLO}[%]	σ_{LO} [fb]	$\sigma_{\mathrm{NLO\,EW}}$ [fb]	δ_{EW}[%]	f_{NLO}[%]
	$\mathrm{b\bar{b}}$, γb, $\gamma\bar{\mathrm{b}}$ excluded				$\mathrm{b\bar{b}}$ included, γb, $\gamma\bar{\mathrm{b}}$ excluded			
full	254.79(2)	249.88(9)	−1.93	103.5	259.02(2)	253.95(9)	−1.96	103.4
unp.	245.79(2)	241.48(2)	−1.75	100	249.97(2)	245.49(2)	−1.79	100.0
LL	18.752(2)	18.510(2)	−1.30	7.7	21.007(2)	20.663(2)	−1.64	8.4
LT	32.084(3)	32.043(3)	−0.13	13.3	33.190(3)	33.115(3)	−0.23	13.5
TL	33.244(5)	33.155(5)	−0.27	13.7	34.352(5)	34.230(5)	−0.35	13.9
TT	182.17(2)	177.83(2)	−2.38	73.6	182.56(2)	178.21(3)	−2.38	72.6
int.	−20.46(3)	−20.1(1)	−1.96	−8.3	−21.14(5)	−20.6(2)	−2.45	−8.4
	$\mathrm{b\bar{b}}$, γb, $\gamma\bar{\mathrm{b}}$ included							
full	259.02(2)	265.59(9)	+2.54	-				

- Including bottom antibottom induced processes enhances the production of longitudinally polarised W bosons
- Diagrams with t channel top quarks
- Top quark predominantly couples to longitudinally polarised W bosons

Integrated results

state	σ_{LO} [fb]	$\sigma_{\mathrm{NLO\,EW}}$ [fb]	δ_{EW}[%]	f_{NLO}[%]	σ_{LO} [fb]	$\sigma_{\mathrm{NLO\,EW}}$ [fb]	δ_{EW}[%]	f_{NLO}[%]
	$\mathrm{b\bar{b}}$, $\gamma\mathrm{b}$, $\gamma\mathrm{\bar{b}}$ excluded				$\mathrm{b\bar{b}}$ included, $\gamma\mathrm{b}$, $\gamma\mathrm{\bar{b}}$ excluded			
full	254.79(2)	249.88(9)	−1.93	103.5	259.02(2)	253.95(9)	−1.96	103.4
unp.	245.79(2)	241.48(2)	−1.75	100	249.97(2)	245.49(2)	−1.79	100.0
LL	18.752(2)	18.510(2)	−1.30	7.7	21.007(2)	20.663(2)	−1.64	8.4
LT	32.084(3)	32.043(3)	−0.13	13.3	33.190(3)	33.115(3)	−0.23	13.5
TL	33.244(5)	33.155(5)	−0.27	13.7	34.352(5)	34.230(5)	−0.35	13.9
TT	182.17(2)	177.83(2)	−2.38	73.6	182.56(2)	178.21(3)	−2.38	72.6
int.	−20.46(3)	−20.1(1)	−1.96	−8.3	−21.14(5)	−20.6(2)	−2.45	−8.4
	$\mathrm{b\bar{b}}$, $\gamma\mathrm{b}$, $\gamma\mathrm{\bar{b}}$ included							
full	259.02(2)	265.59(9)	+2.54	-				

- Sizeable contribution from the interference of longitudinally and transversely polarised W bosons
- Transverse momentum cuts on the charged leptons prevent the cancellation of the interferences

Positron decay angle $\cos\left(\vartheta^{*,\mathrm{CM}}_{e^+}\right) = \frac{\vec{p}^{\,*}_{e^+} \cdot \vec{p}^{\,\mathrm{CM}}_{e^+\nu_e}}{|\vec{p}^{\,*}_{e^+}||\vec{p}^{\,\mathrm{CM}}_{e^+\nu_e}|}$

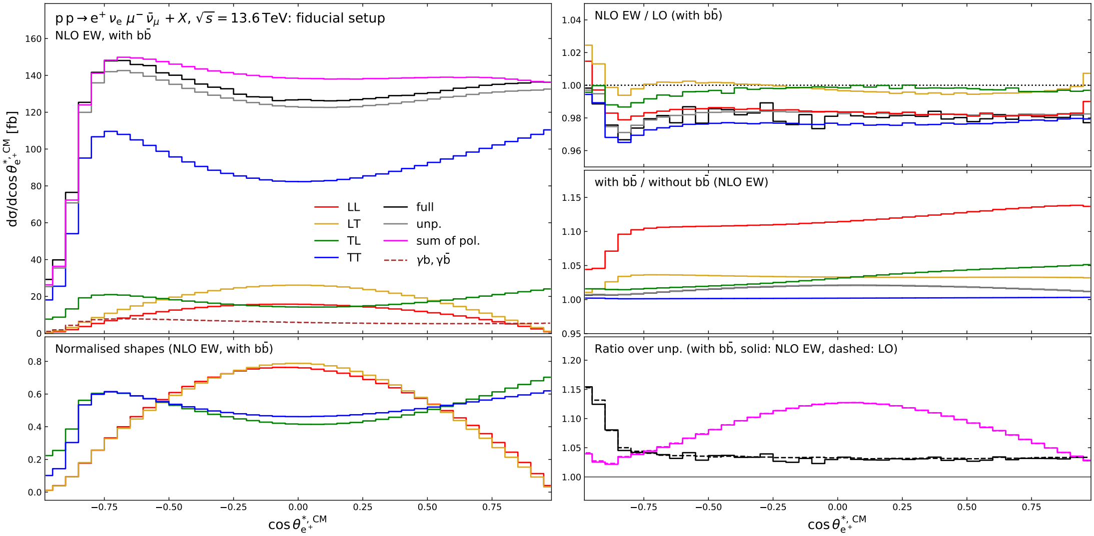

Positron decay angle $\cos\left(\vartheta^{*,\mathrm{CM}}_{e^+}\right) = \frac{\vec{p}^{\,*}_{e^+} \cdot \vec{p}^{\,\mathrm{CM}}_{e^+\nu_e}}{|\vec{p}^{\,*}_{e^+}||\vec{p}^{\,\mathrm{CM}}_{e^+\nu_e}|}$

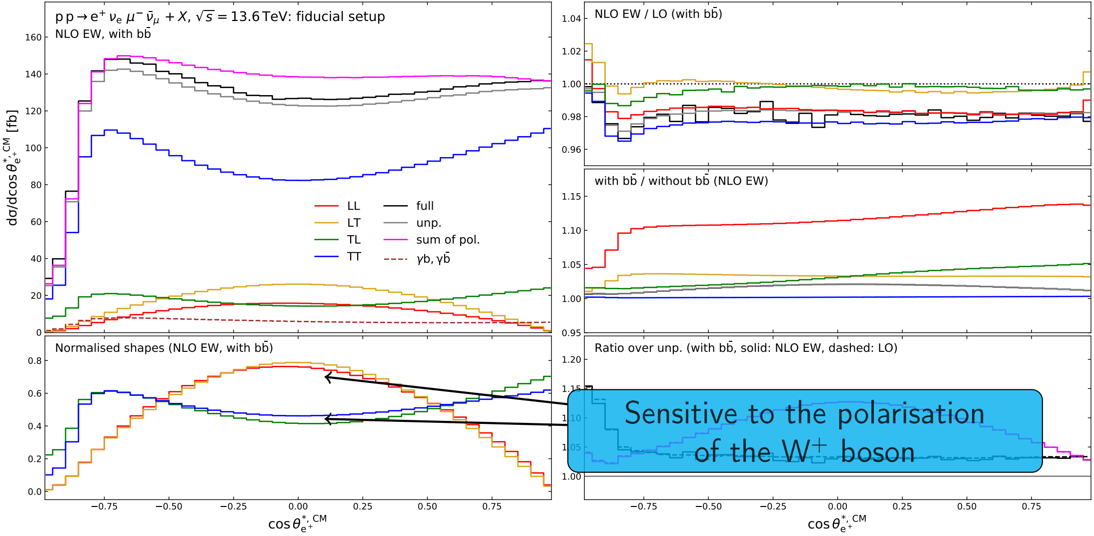

Positron decay angle $\cos\left(\vartheta^{*,\mathrm{CM}}_{e^+}\right) = \frac{\vec{p}^{\,*}_{e^+} \cdot \vec{p}^{\,\mathrm{CM}}_{e^+\nu_e}}{|\vec{p}^{\,*}_{e^+}||\vec{p}^{\,\mathrm{CM}}_{e^+\nu_e}|}$

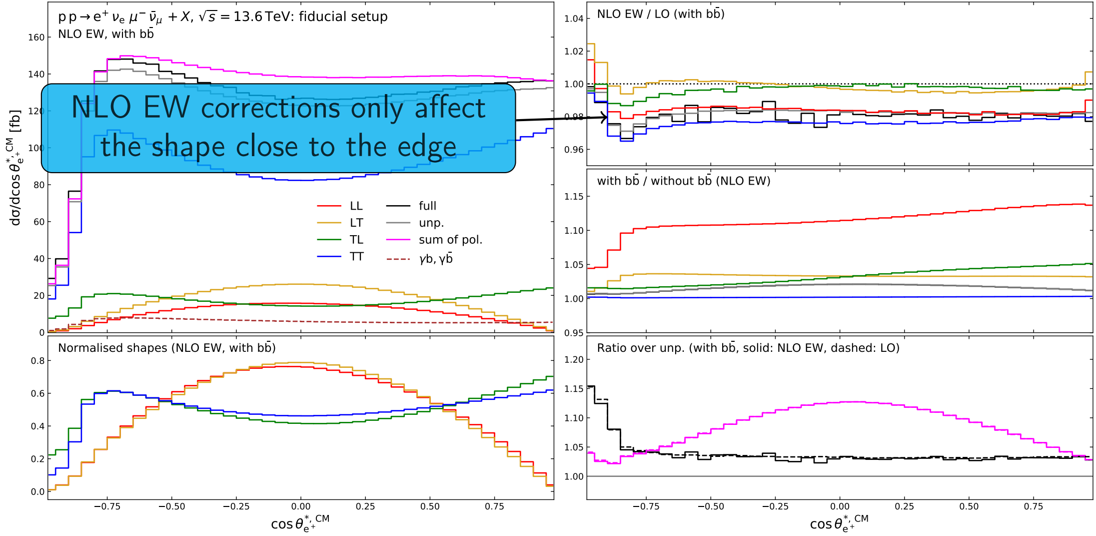

NLO EW corrections only affect the shape close to the edge

Positron decay angle $\cos\left(\vartheta^{*,\mathrm{CM}}_{e^+}\right) = \frac{\vec{p}^{\,*}_{e^+} \cdot \vec{p}^{\,\mathrm{CM}}_{e^+\nu_e}}{|\vec{p}^{\,*}_{e^+}||\vec{p}^{\,\mathrm{CM}}_{e^+\nu_e}|}$

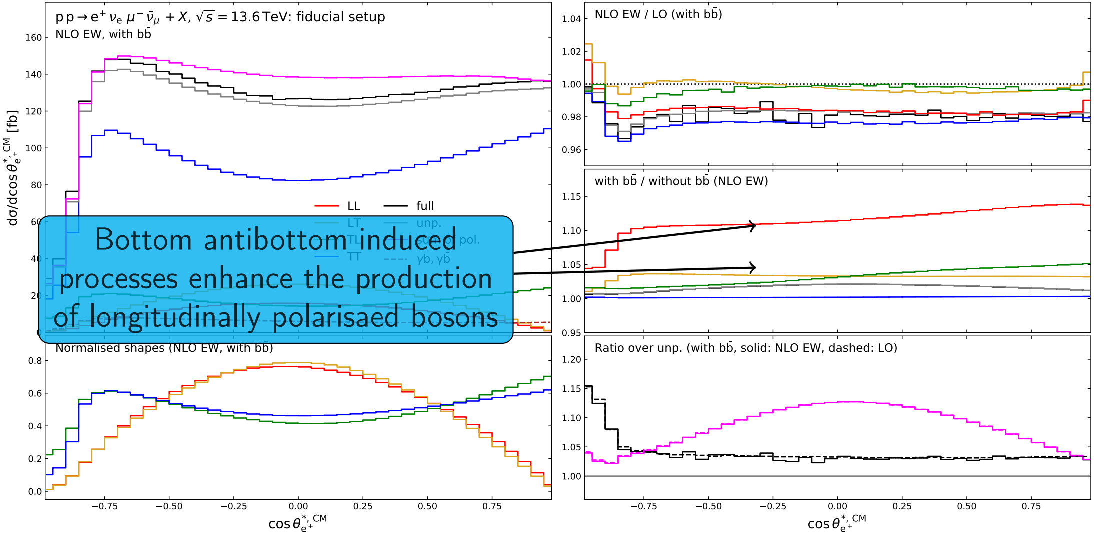

Invariant mass positron and muon $M_{e^+\mu^-} = (p_{e^+} + p_{\mu^-})^2$

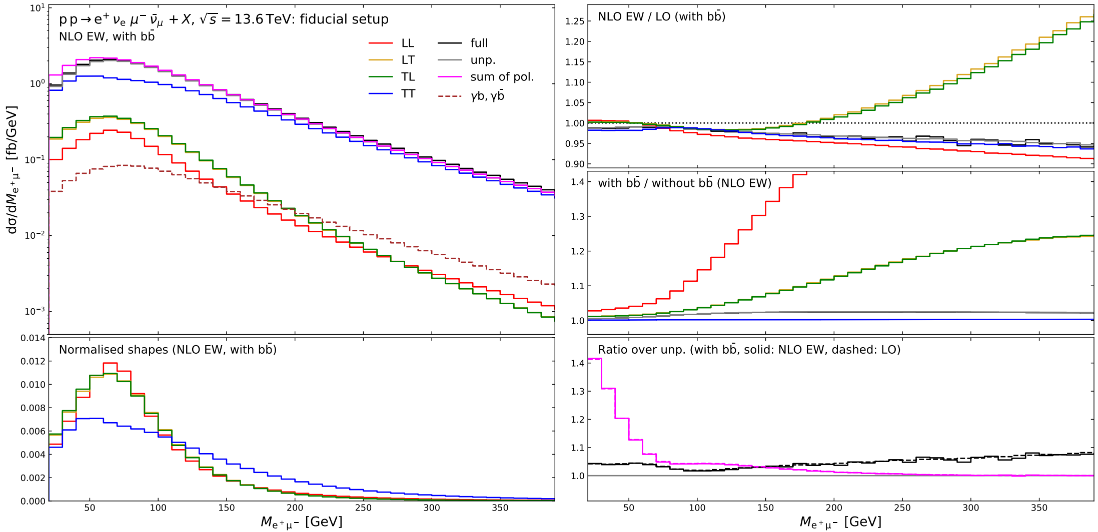

Invariant mass positron and muon $M_{e^+\mu^-} = (p_{e^+} + p_{\mu^-})^2$

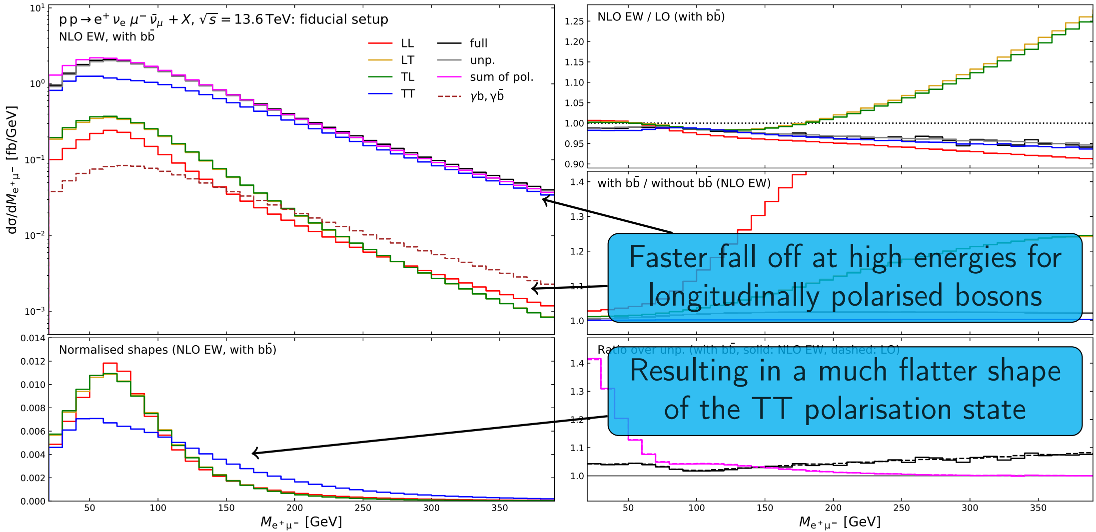

Invariant mass positron and muon $M_{e^+\mu^-} = (p_{e^+} + p_{\mu^-})^2$

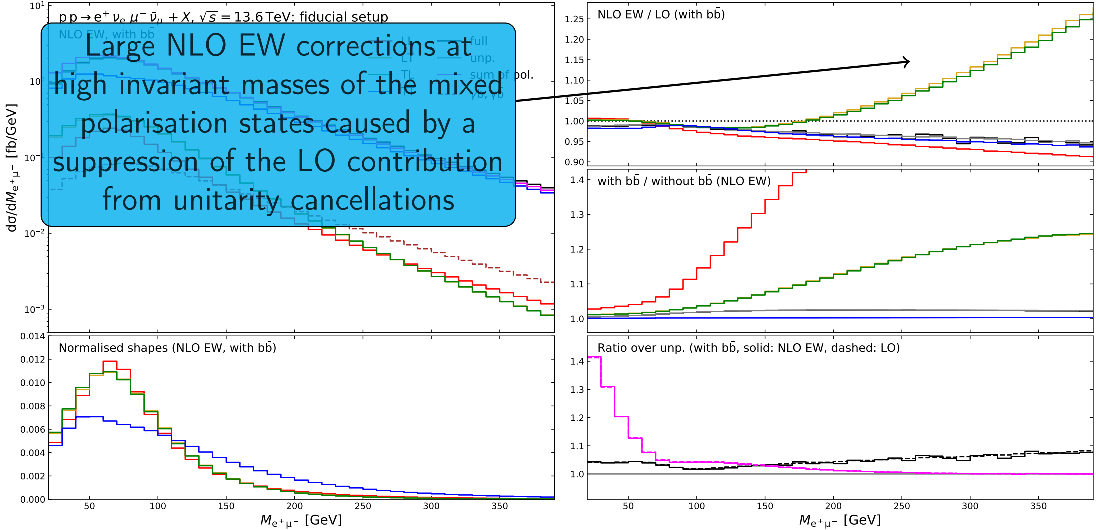

Invariant mass positron and muon $M_{e^+\mu^-} = (p_{e^+} + p_{\mu^-})^2$

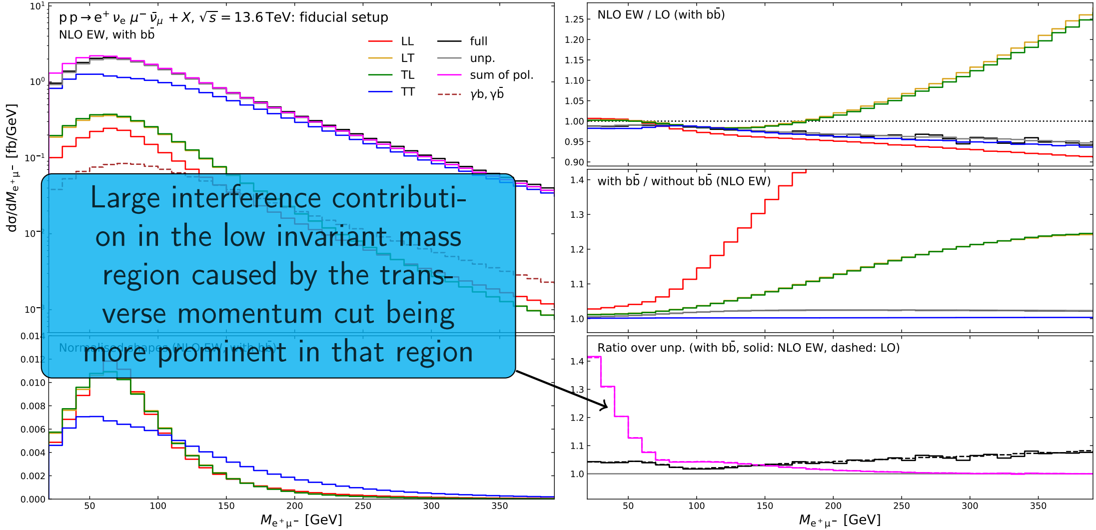

Large interference contribution in the low invariant mass region caused by the transverse momentum cut being more prominent in that region